Journal of Computational Physics **157,** 120–142 (2000)
doi:10.1006/jcph.1999.6366, available online at http://www.idealibrary.com on IDEAL®

# A Computational Study of Rising Plane Taylor Bubbles

Prabir Daripa

*Department of Mathematics, Texas A&M University, College Station, Texas 77843*

Received April 5, 1999

The problem of a plane bubble rising in a 2-D tube is revisited using Birkhoff's formulation developed in 1957. The equations in this formulation have a one parameter (Froude number $F$) family of solutions which are divided into three regimes characterized by distinct topologies at the apex. These equations are solved numerically using a conventional series representation method and Newton's iterations. This numerical method fails for values of $F$ in a range which contains the transition points. In this paper, it is demonstrated through careful numerical computations how and why this method fails. We also analyze the series and provide estimates of the transition points. This strategy of estimating the transition points can be used for some problems where the conventional series representation method fails because it does not adequately account for changes in the nature of the singularity that takes place as these transition points are approached in the parameter space. Furthermore, existence of two new critical Froude numbers is demonstrated numerically. We further show that the previous results on this problem have been incomplete by leaving out the characterization of the topology at the apex of the bubbles for values of $F$ in the regime $0.234 < F < 0.3578$. We also resolve this issue in this paper. 

## 1. INTRODUCTION

The planar interface between a heavy and a light fluid under gravitational acceleration is known to be an equilibrium configuration of fluid flow equations. This interface is known to be unstable (stable) if an accelerating force, such as gravity, is directed from the heavy (light) fluid to the light (heavy) fluid. This instability is known as the Rayleigh–Taylor (RT) instability, and it plays an important role in many practical situations including inertial confinement fusion, astrophysical jets, two phase flows and fluidized bed. One of the many possible asymptotic scenarios in the late stages of RT instability is the steady state motion of a periodic array of bubbles [11, 27]. A useful model to capture some essential features of this scenario is an infinitely long plane bubble rising in a gravity field through an incompressible and inviscid fluid. The bubble profile is symmetric about the centerline of the channel and approaches the channel walls asymptotically at far downstream.



0021-9991/00 $35.00

This problem is mathematically characterized by two parameters: (i) the included angle, $\theta_t$, at the apex of the bubble; and (ii) the dimensionless speed, $F = U/\sqrt{gh}$ (Froude number) where $U$ is the actual speed of the bubble, $g$ is the gravity and $h$ is the width of the two-dimensional tube. Admissible values of $\theta_t$ according to the theory are $180^\circ$, $120^\circ$, and $0^\circ$ corresponding to smooth, pointed, and cusped bubbles, respectively [9, 13, 28, 30]. Below, we will encounter three critical values of Froude numbers: $F_1 = 0.234$, $F_C = 0.3578$, $F_2 = 0.8$. The relevance of these speeds will be made clear.

Due to the awkward nonlinearity of the problem, a combination of asymptotic analyses and numerical computation [2–4, 10, 13, 28, 30] has been used in the past to address the question of admissible values of speed of these bubbles. Most of the early numerical works have been based on conformal mapping and the series expansion method [4, 30]. Later, similar calculations have been carried out using the real-space boundary integral approach [7, 19]. Most of the numerical results obtained by these methods have been found to be consistent with each other.

The theoretical and numerical works of Birkhoff and Carter [4] and the theoretical work of Garabedian [13] in the late fifties suggest that there is a continuum family of smooth bubbles rising at a speed of $F \leq F_s$, where $F_s$ refers to the speed of the fastest smooth bubble. Approximate asymptotic analysis of Garabedian [13] puts the estimate of this speed $F$ at an approximate value of 0.24. More recent computations [8, 28] which use conformal-mapping and the Fourier collocation method have provided numerical evidence to the fact that a bubble with a stagnation point at its tip can rise at any speed $F \leq F_C$. Since these bubbles could be smooth or pointed, Garabedian [14] conjectured that these bubbles for values of $F > F_1$ are probably pointed bubbles. Later numerical calculations of Vanden-Broeck [30] and Daripa [10] obtained a pointed bubble only at $F = F_C$. There are no well-documented data regarding the nature of the topology at the apex for bubbles in the approximate regime $F_1 < F < F_C$. It has been speculated that these bubbles may as well be legitimate pointed bubbles [14, 15]. Thus it appears that a careful study is required to properly characterize solutions in the regime: $F_1 < F < F_C$. To this end, we would like to mention that these observations are also consistent with numerical results obtained using the real space boundary integral approach [7, 19].

In this paper,

- we investigate the topology of the bubbles in the regime $F_1 < F < F_C$ and characterize these bubbles as smooth bubbles;
- we sketch a transition scenario from smooth to pointed and pointed to cusped bubbles and attribute certain numerical difficulties to the delicate nature of the singularity in the complex velocity at the tip and the transition phenomenology;
- one of the numerical observations made during our computations with a specific series representation of the solution is the existence of a threshold phenomenon, i.e., swift emergence of oscillations in the Fourier spectra of the numerical solutions as soon as the Froude number exceeds a threshold value of $F_1$ for smooth bubbles and decreases below a threshold value of $F_2$ for cusped bubbles. The possible source of this phenomenon is discussed and relevance of these Froude numbers is indicated;
- our research provides a general idea that is viable for some problems in which conventional series representation methods fail in computing approximate values of the transition points where topology changes occur.
- we provide some interesting results for cusped bubbles.

The paper is laid out as follows. In Section 2, we briefly review the formulation of the problem. We discuss some relevant theoretical and computational issues in Section 3. Issues of topological transition are addressed in Section 4. In Section 5 we provide some validation criteria. Numerical results that are necessary for our purposes mentioned above are presented in Section 6. A sketch of topological transition is suggested in Section 7. Finally we conclude and discuss some open problems in Section 8.

## 2. PRELIMINARIES

The formulation of the problem and the numerical approach have been discussed in Daripa [10] and are almost identical to Birkhoff and Carter [4] and Vanden-Broeck [28]. Analysis to be presented in Section 3 and discussion of the results to be presented in later sections require that we present a very brief outline of the formulation and the numerical method here.

With respect to the reference frame attached to the bubble, the fluid upstream in a tube of width $h$ has a speed $U$ downward. With appropriate normalization (speed by $U$ and time by $(\frac{h}{U})$), far upstream (i.e., $x \to -\infty$) $q = 1, \theta = 0$, where $q$ is the speed and $\theta$ is the flow direction. The apex of the bubble is located at $x = y = 0$. It is useful to deal with this problem in an auxiliary circle plane, $|\sigma| \le 1$, which is obtained by a conformal mapping of the potential plane image of the flow in the physical plane. This maps the bubble surface onto the upper semi-circle $\sigma = e^{i\alpha}$, $\alpha \in [0, \pi]$, the walls on $(-1, 1)$ and the flow domain onto the interior of the domain bounded by the upper semi-circle and the real axis. The image of the apex of the bubble is $\sigma = i$ and that of the tail of the bubble is $\sigma = \mp 1$.

The complex function $\tau = \nu - i\theta$, where $\nu = \ln q$, is an analytic function of $\sigma$ within the semi-circle and satisfies the symmetry condition $\tau(\sigma) = \overline{\tau}(-\overline{\sigma})$ due to symmetry of the bubble surface about the centerline of the tube (see Fig. 1). In the above, an overbar denotes complex conjugacy. Moreover, since $\tau(\sigma)$ is continuous and real on the real axis (since $\theta = 0$ on real axis, the image of the walls), it also satisfies the condition $\tau(\sigma) = \overline{\tau}(\overline{\sigma})$, in $|\sigma| \le 1$, by Schwartz reflection principle. As discussed in detail by Birkhoff [2–4], the asymptotic behavior of $\tau$ at the tail($\sigma = \mp 1$) and the apex($\sigma = i$) of the bubble are given by

$$e^{\tau} \approx [-\ln C(1-\sigma^2)]^{1/3}, \quad \text{as } \sigma \to \mp 1; \qquad e^{\tau} \approx (1+\sigma^2)^{\gamma}, \quad \text{as } \sigma \to i, \tag{2.1}$$

where $\gamma = \theta_t/\pi \ge 0$ with $\theta_t$ as the included angle of the bubble at the apex.

An appropriate representation of $\tau(\sigma)$ in $|\sigma| \le 1$ which satisfies all the above conditions is then given by

$$e^{\tau(\sigma)} = (1+\sigma^2)^{\gamma}[-\ln C(1-\sigma^2)]^{1/3}[-\ln C]^{-1/3} e^{g(\sigma;\theta_t)}, \tag{2.2}$$

with

$$g(\sigma;\theta_t) = \sum_{n=1}^{\infty} a_n(\theta_t)\sigma^{2n}, \tag{2.3}$$

where $0 < C < 0.5$ and the Fourier coefficients, $a_n$, are real. Since the values of these Fourier coefficients depend on the value of $\theta_t$, we have explicitly shown this here using the notation $a_n(\theta_t)$. Explicit dependence of these coefficients on $F$ is suppressed from this notation. A

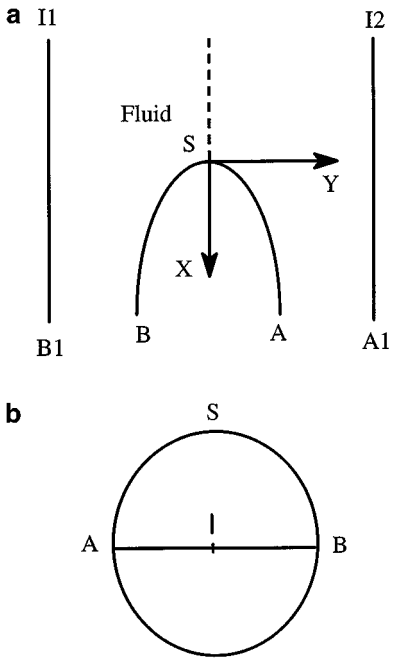


**FIG. 1.** (a) The physical region: a bubble is rising upward in the fluid with speed $U$. The diameter of the tube is $h$; (b) The circle plane is $|\sigma| \leq 1$.

derivative form of the Bernoulli's equation on the bubble interface in this circle plane is given by [9]

$$\pi \tan\alpha e^{2\nu} \frac{d\nu}{d\alpha} + \frac{e^{-\nu}}{F^2} \cos\theta = 0, \qquad 0 \leq \alpha < \frac{\pi}{2}. \tag{2.4}$$

In the Fourier collocation method [28], expressions for $\nu, \theta$, and their derivatives from (2.2) are substituted in (2.4). This gives an equation containing $F, \gamma$, and an infinite number of Fourier coefficients $a_n$. In order to solve it numerically, only a finite number of Fourier coefficients are retained and Eq. (2.4) is applied at $N$ equi-spaced points: $\alpha_I = (\pi/2N)(I - 1/2)$, $I = 1, \ldots, N$. This gives a system of $N$ number of nonlinear equations. If $\gamma$ is prescribed, then the Fourier series is truncated after $N$ terms and the equations are solved by Newton's iterations for $N$ number of unknown Fourier coefficients. If $\gamma$ is not prescribed, then the Fourier series is truncated after $N-1$ terms and the equations are solved by Newton's iterations for $\gamma$ and $N-1$ number of unknown Fourier coefficients. Numerical convergence for a choice of $N$ is achieved if the values of the unknowns do not change more than $10^{-8}$ between two successive Newton iterations. Once this is solved, values of $q$ and $\theta$ at mesh points are obtained from (2.2). Numerical solutions are obtained in this fashion for an increasing sequence of values of $N$ to test for convergence of the $N$ unknown Fourier coefficients and of the bubble profiles generated from integrating the equation

$$z_\alpha = -\frac{\cot\alpha}{\pi q} e^{i\theta}, \qquad 0 \leq \alpha \leq \pi, \tag{2.5}$$

where $z = x + iy$.

The series representation (2.2) is not unique. For example, consider the following which is similar to the one used by Vanden-Broeck [28],

$$e^{\tau(\sigma)} = [-\ln C(1-\sigma^2)]^{1/3}[-\ln C]^{-1/3}(1+h(\sigma;\theta_t)). \tag{2.6}$$

This representation works well for finding bubbles with or without stagnation point (see [28]). Since the flow direction $\theta$ is discontinuous at a stagnation point, computed values of $\theta$ using series representation (2.3) for $h$ in (2.6) will have poor accuracy, in particular near the stagnation point, due to Gibbs' phenomenon. Therefore, conclusions about the topology at the apex based on direct estimate of the apex angle $\theta_t$ from these computed values may be misleading.

The advantage of using (2.2) as opposed to using (2.6) lies in the ability to detect presence or absence of pointed bubbles and smooth bubbles. We discuss this in Sections 3 and 4.

*Remark 1.* The end points (i.e., the tail and the tip of the bubble) cannot be used as collocation points because the variable $\nu = \ln q$ in (2.4) diverges at these points.

*Remark 2.* Since the collocation points closest to the end points approach these points as $N \to \infty$ and $\nu$ diverges there, the numerical solutions can be reliable only up to a certain maximum value of $N$. In fact, the scheme will fail for very large values of $N$ because the variable $\nu$ and entries in the derivative matrix required during Newton's iteration would be large and may cause quantities of interest during computation to underflow or overflow. Therefore convergence of the scheme cannot be tested in the strict sense under grid refinement and such a conclusion has to be drawn from calculations for modest values of $N$.

## 3. THEORETICAL AND COMPUTATIONAL ISSUES

A numerical procedure for finding all possible solutions is to use the above scheme for a sequence of positive values $F > 0$ with allowable values of $\theta_t$ in (2.2). As discussed in Daripa [9], these allowable values of $\theta_t$ are $180^\circ$, $120^\circ$, and $0^\circ$. Various works in the literature [4, 10, 13, 28, 30] suggest that there is only one value, $\theta_a$, of $\theta_t$ corresponding to each $F$. Numerical solutions with prescribed values of $\theta_t$ and $F$ which are not consistent (i.e., $\theta_t \neq \theta_a$) may appear reasonable at times unless Fourier spectra of the solutions are carefully scrutinized as discussed below.

If computations use $\theta_t \neq \theta_a$, then the function $g(\sigma;\theta_t)$ in (2.2) will diverge logarithmically at the stagnation point and the series (2.3) for this function will converge only for $|\sigma| \leq 1$, $\sigma \neq \mp i$. To be precise, we have from (2.2)

$$g(\sigma;\theta_t) = g(\sigma;\theta_a) + \epsilon \ln(1+\sigma^2); \qquad |\sigma| \leq 1, \tag{3.1}$$

where $\epsilon = (\theta_a - \theta_t)/\pi$. The Taylor series of $g(\sigma, \theta_t)$ will now converge only for $|\sigma| \leq 1$, $\sigma \neq \mp i$, because of the logarithmic branch point at $\sigma = i$. The Taylor series

$$\ln(1+\sigma^2) = \sum_{n=1}^{\infty} \frac{(-1)^{n+1}}{n} \sigma^{2n}, \tag{3.2}$$

for the logarithmic term in (3.1) converges slowly, in fact very slowly, at points in the neighborhood of $\sigma = \mp i, \mp 1$ and also at $\sigma = \mp 1$. Because of this and the two previous

remarks made in Section 2, it is possible to obtain numerical solutions with modest values of $N$ even if $\theta_t \neq \theta_a$ (see Daripa [9]). In that case, the numerically generated bubble will have neither the correct apex angle, $\theta_a$, due to Gibbs' phenomenon nor the prescribed angle $\theta_t$.

However, such spurious solutions can be detected by carefully analyzing the series (2.3) for $g(\sigma;\theta_t)$ given by (3.1). Since the spurious solutions are associated with the presence of logarithmic singularities on the unit circle (see Eq. (3.1)), it would seem appropriate to identify such solutions by analyzing the pattern of signs in the series which are determined by the singularities on the radius of convergence. For example, the pattern of signs in the series (3.2) is alternating due to the presence of singularities at $\sigma^2 = -1$. When the pattern of signs is alternating or fixed, Cauchy's ratio test is the most useful in the graphical form devised by Domb and Sykes [12] to determine the radius of convergence and, in some instances, also the nature of the singularities. Van-Dyke [31] gives a lucid account with many examples of how the pattern of signs in the series is determined by the singularities.

For some series, the final pattern of signs determined by the singularity may appear after only a few terms and for others, it may appear after many terms. In the latter case, the singularity may not be detected easily unless enough terms in the series are available. This is illustrated by

$$(1+\epsilon)^p = 1 + p\epsilon + \frac{p(p-1)}{2}\epsilon^2 + \frac{p(p-1)(p-2)}{6}\epsilon^3 + \cdots, \tag{3.3}$$

where $p > 0$ is not an integer. The larger the value of $p$, the larger would be the number of terms after which the pattern of signs determined by the singularity appears. An example which is more relevant to the current problem is illustrated by

$$\ln(1+x) = \sum_{n=1}^{\infty} \frac{(-1)^{n+1}}{n} x^n, \tag{3.4}$$

where the pattern of signs determined by the singularity on the radius of convergence appears right from the beginning of the series. On the other hand, the series $\sum_{n=1}^{\infty}(x^n/n^p)$, $p > 1$, converges for all $|x| \leq 1$. Now consider the series

$$S(x) = \sum_{n=1}^{\infty} \frac{x^n}{n^p} + \epsilon \sum_{n=1}^{\infty} \frac{(-1)^{n+1}}{n} x^n = \sum_{n=1}^{\infty} \left( \frac{1}{n^p} + \epsilon \frac{(-1)^{n+1}}{n} \right) x^n, \tag{3.5}$$

which converges for $-1 < x \leq 1$ and has a singularity at $x = -1$. Analysis of this series for $S(x)$ is more subtle because the pattern of signs determined by the singularity at $x = -1$ may not appear soon enough unless $\epsilon$ in (3.5) is not very small. For example, the pattern of alternating signs that was present right from the beginning in the series for $\ln(1+x)$ in (3.4) appears in the modified series (3.5) only after $(1/\epsilon^{p-1})$ number of terms which is very large for small values of $\epsilon$ (remember $p > 1$). However, this modified series (3.5) displays a pattern of oscillations starting from the first few terms precisely due to this same singularity on the circle of convergence.

Therefore, analysis of the series for $g(\sigma,\theta_t)$ is more subtle because the pattern of signs determined by the singularities in (3.1) may not appear early in the series for small values of $\epsilon$. The spurious solutions, however, can be determined by the presence of oscillations in the Fourier spectrum which signals the presence of singularities on the unit circle. This is discussed in the next section in the context of the bubble problem.

3.1. *Analysis of the Series*

Equations (3.1) and (3.2) imply that nonzero values of $(\theta_t - \theta_a)$ should change the behavior of the series (2.3) in a way that is consistent with the series (3.2). It is evident from (3.2) that this will leave a qualitative imprint on the Fourier spectra of the numerical solutions. To be precise, it follows from (2.3), (3.1), and (3.2) that the series coefficients $a_n(\theta_t)$ $a_n(\theta_a)$ are related by

$$a_n(\theta_t) = a_n(\theta_a) + \epsilon \frac{(-1)^{n+1}}{n}, \qquad n = 1, \ldots, \infty. \tag{3.6}$$

Since $g(\sigma, \theta_a)$ is bounded and continuous on the unit circle, the most conservative estimate of the asymptotic behavior of $a_n(\theta_a)$ is given by

$$a_n(\theta_a) = o\left(\frac{1}{n}\right), \qquad \text{as } n \to \infty. \tag{3.7}$$

Therefore Eq. (3.6) becomes

$$a_n(\theta_t) \sim \epsilon \frac{(-1)^{n+1}}{n}, \qquad \text{as } n \to \infty, \tag{3.8}$$

indicating that amplitudes of the coefficients $a_n(\theta_t)$ for a choice of $\theta_t \neq \theta_a$ will alternate in sign from odd to even $n$ and will slowly decay to zero as $n \to \infty$. However, in practice the series is truncated which has the following implications for our purposes here. If

$$a_n(\theta_a) \sim K n^{-p}, \qquad \text{as } n \to \infty, \tag{3.9}$$

with $K > 0$ and $p$ greater than but close to one ($p$ appears to be in the range $1.3 \leq p \leq 1.4$ for most of the bubble solutions), then it follows from (3.6) that $a_n(\theta_t)$ for choices of $\theta_t \neq \theta_a$ will decay with oscillations at large wavenumbers but may not alternate in sign (from odd to even $n$) unless $\epsilon$ is not very small. In other words, persistent oscillations in the Fourier spectra as $n \to \infty$ and slow decay rate according to Eq. (3.8) are the only important indicators of spurious solutions. Moreover, Eq. (3.6) suggests that such oscillations will appear in the entire Fourier spectrum $a_n(\theta_t)$ if $a_n(\theta_a)$ decays monotonically with $n$. It is perhaps useful at this point to exemplify these observations.

It is well established [4, 10, 13, 28, 30] that a smooth bubble exists when $F = 0.23$ and a pointed bubble exists at $F = 0.3578$. We show some results with these values of $F$.

Figure 2 shows some graphs taken from our computed solutions at $F = 0.23$ and two different values of $\theta_t$: $180^\circ$, $178^\circ$. Figure 2a depicts surface profiles (only the left half) of these numerically generated bubbles for these two values of $\theta_t$ and $F = 0.23$. These profiles near the tails are indistinguishable and satisfy the asymptotic shape of these bubbles near the tails. Figure 2b depicts a magnified view of the regions around the tips of the bubbles in Fig. 2a. It is reasonable to conclude from the thousandfold magnification of the $y$ axis in this plot that these profiles agree exceedingly well. The Fourier modal amplitudes decay monotonically when $\theta_t = 180^\circ$. This is shown in Fig. 2c. Figure 2d shows the magnitude of Fourier coefficients against the wavenumber when $\theta_t = 178^\circ$. The Fourier modal amplitudes in this case are initially (up to fifth wavenumber) large compared to the Fourier coefficients of the logarithmic term (see (3.2)) and, hence, the beginning part of the spectrum (up to fifth

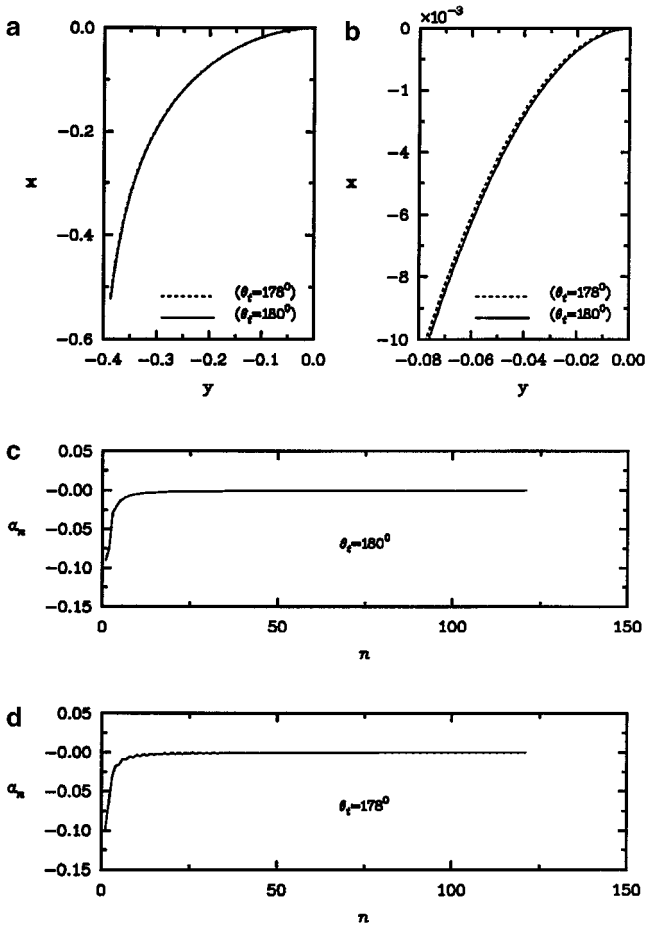


**FIG. 2.** Effect of small variation in the apex angle with $F = 0.23$ and $N = 121$: (a) Comparison of bubble shapes; (b) magnified view of the bubble profiles near the tip; (c) Fourier coefficients with $\theta_t = 180^\circ$; (d) Fourier coefficients with $\theta_t = 178^\circ$.

wavenumber) does not have any oscillations. Thereafter, oscillations in the Fourier spectrum are clearly visible in the plot because the transients introduced by the logarithmic branch point now dominate the spectrum. Amplitude of these oscillations decreases with increasing wavenumber and is too small to be detected visually for high wavenumbers in this plot.

Figure 3 shows results of numerical experiments for $F = 0.35784$ and two different values of $\theta_t$: $120^\circ$, $118^\circ$. In Figs. 3c and 3d, smooth (monotonic) and oscillatory Fourier spectra are clearly recognizable, a clear indication that the oscillations arise because $\theta_t$ does not correspond to the correct value $120^\circ$. The amplitude of oscillations in both the figures is very mild because $\epsilon$ ($\frac{2*\pi}{180} = 0.0349$) is very small (see (3.8)). We have found that amplitude of such oscillations in the Fourier spectrum increases with $|\theta_a - \theta_t|$ (i.e., the difference between the correct tip angle and the specified value of $\theta_t$ used during computations) which is consistent with our analysis above.

*The analysis and calculations presented above lead us to surmise that persistence of oscillations in the Fourier spectrum as $n \to \infty$ may indicate that the value of $\theta_t$ used for computation is not the correct apex angle of the bubble solution at that value of $F$. It is worth pointing out that this conclusion does not follow if one uses representation* (2.6) *instead of* (2.2).

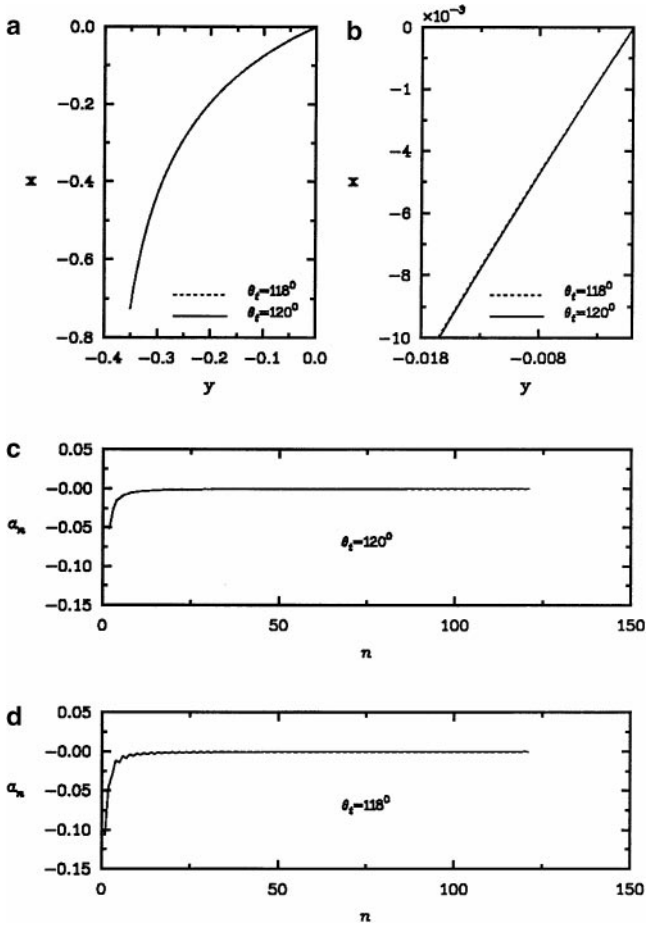


**FIG. 3.** Effect of variation in the apex angle with $F = 0.35784$ and $N = 121$. (a) Comparison of bubble shapes; (b) magnified view of the bubble profiles near the tip; (c) Fourier spectrum when $\theta_t = 120^\circ$; (d) Fourier spectrum when $\theta_t = 118^\circ$.

We measure the extent of such oscillations by monitoring the number of times the plot of $a_n$ versus $n$ changes trend (from decrease to increase or decrease to increase) as a fraction of the total number of Fourier coefficients used in the calculation. For lack of a better name, we call this ratio the frequency of oscillations and use the abbreviation fos for it occasionally. We should note from our discussion so far in this section that the limiting (as $N \to \infty$) value of this ratio fos should be one if there indeed is a logarithmic singularity (however weak, i.e., regardless of how small the $\epsilon$ is in Eq. (3.1)) on the radius of convergence of the series. Since presence of this singularity is synonymous with spurious solutions, such solutions can be determined by estimating the limiting values of fos. We will show below that this test is most useful in a graphical format to detect such spurious solutions.

## 4. TOPOLOGICAL TRANSITION AND SINGULARITIES

It is not difficult to see from (2.2) that behavior of the function $g(\sigma\,;\theta_t)$ in the neighborhood of the tip has to be very complicated so that the complex velocity develops singularity of the right order as the topological transition (smooth to pointed and pointed to cusped bubbles)

takes place at certain values of $F$. In particular, if there are smooth bubbles for $F < F_l$, pointed bubbles for $F_l \le F \le F_u$, and cusped bubbles for $F > F_u$, then it follows from (2.2) that

$$g(\sigma;\pi) \to -\frac{1}{3}\ln(1+\sigma^2) + g\left(\sigma;\frac{2\pi}{3}\right), \qquad \text{as } F \uparrow F_l, \tag{4.1}$$

and

$$g(\sigma;0) \to -\frac{2}{3}\ln(1+\sigma^2) + g\left(\sigma;\frac{2\pi}{3}\right), \qquad \text{as } F \downarrow F_u, \tag{4.2}$$

where $g(\sigma;\pi)$, $g(\sigma;2\pi/3)$, and $g(\sigma;0)$ are all bounded functions in $|\sigma| \le 1$. Below we provide numerical results which indicate that $F_l = F_u = F_C$. This means that the function $g(\sigma;\theta_t)$ has to develop logarithmic branch points of different order at the tip of the pointed bubble depending on whether the pointed bubble is approached from below or above $F_C$. Therefore, behavior of the function $g(\sigma;\theta_t)$ has to be complicated for values of $F$ close to $F_l$ and $F_u$ which are not adequately accounted for in (2.3).

## 5. DIAGNOSTIC TOOLS

### 5.1. *Asymptotic Shape*

The asymptotic shape of the bubble interface for large $x$ downstream is given by (see [28])

$$x = F^2/2(1-2y)^2. \tag{5.1}$$

### 5.2. *Tip Angle*

It follows from Section 2 that the tip angle $\theta_a$ is related to the flow variables $\theta$ and $q$ and their derivatives at the tip by the relations

$$\theta(\beta = 0^+) = -\frac{\theta_a}{2} \tag{5.2}$$

and

$$\frac{\pi F^2}{3} = (q^3)_{\beta\beta}|_{\beta\to 0} = \cos\left(\frac{\theta_a}{2}\right). \tag{5.3}$$

Above we have used $\beta = \frac{\pi}{2} - \alpha$ and, hence, $\beta = 0$ corresponds to the tip of the bubble. Equation (5.2) is very obvious and can be viewed as the definition of the tip angle. The relation (5.3) arises from rewriting the interface condition (2.4) at the tip of the bubble and has been discussed in some detail in Daripa [9].

Use of the relations (5.2) and (5.3) is very limited here and, in fact, should not be used for validation purposes because it is difficult to accurately compute the values on the left hand sides of these equations. It is worth mentioning here the numerical method does not even use the apex as a collocation point. We have also verified our contention in known cases and found that these relations should not be used for purposes of validating whether numerical solutions have the prescribed values of the apex angle or not. Instead, we should use our main result given in the next section.

### 5.3. *Properties of the Fourier Spectrum*

From our discussion in Section 3 and well known facts from the literature on Fourier series [32], we state the following two propositions in relation to numerical solutions with representation (2.2).

PROPOSITION 1. *If $\theta_t$ used in computation is the correct angle at the tip, then $a_n \sim o(1/n)$ as $n \to \infty$.*

PROPOSITION 2. *A sufficient condition for the emergence of oscillations in the Fourier spectrum of a solution at a given $F$ as $n \to \infty$ is that the value of $\theta_t$ used for computation be different from the correct tip-angle $\theta_a$.*

Below we refer to the following as our main result which follows from Proposition 2. *Absence of persistent oscillations in the values of $a_n$ at large $n$ as $n \to \infty$ indicates that the corresponding solution is the correct solution, i.e., the apex angle of the solution at that value of $F$ must be the value of $\theta_t$ used for computation.*

Our main result can be used to validate that a numeral solution at a certain value of $F$ has an apex angle equal to the value of $\theta_t$ used for computation. For this, it is necessary to scrutinize the qualitative asymptotic behavior of the Fourier spectra as $N \to \infty$. As we will see in Section 6, this is to be inferred here from observing the trend in the behavior of the Fourier spectra of the solutions obtained from using a sequence of modest values of $N$.

## 6. NUMERICAL RESULTS

Numerical experiments have been carried out with several values of $N$ up to 251 for various values of $F$ in the regime $0 < F \leq 1$. For brevity, numerical results will be presented for one or more of the following values of $N$: 31, 121, and 251.

We have made some numerical observations which are discussed below. Some of the crucial inferences for values of $F$ in a certain regime have to be drawn in the limit $N \to \infty$ from numerical results. Since numerics are rarely mathematical proofs, it would seem desirable to assemble some relevant numerical results in one place where these might be more accessible to other investigators for comparison with solutions obtained by other numerical and analytical methods. With this in mind, we have depicted some of our numerical results below.

### 6.1. *Pointed Bubbles*

Numerical experiments have been carried out in Daripa [10] with $\theta_t = 120^\circ$ and several values of $F$ between 0 and 1. Daripa [10] (see also Vanden-Broeck [30]) has shown that a legitimate pointed bubble exists at $F = F_C$ and that the Fourier modal amplitudes decay monotonically only at this value of $F$. (This bubble profile is shown later in Section 7). Moreover, Daripa [10] has shown that $a_n \sim n^{-1.35}$ at large wavenumbers. Oscillations develop in the Fourier spectra of the solutions for values of $F$ away from this value (see [10] for more details). It will be helpful to show this behavior in a graphical format devised by Daripa [10]. We show this in Fig. 4. Figure 4b is a magnified view of Fig. 4a in the transition region which shows a very small window in $F$ with no oscillations in the spectrum and the size of this window shrinks to zero with $N \to \infty$. If the interval of this window is $(F_{\min}, F_{\max})$, then a plot of $F_{\min}$ vs $\frac{1}{N}$ in Fig. 4c shows that the Fourier spectra of bubbles away from $F = 0.3784$ will have persistent oscillations as $n \to \infty$. Therefore, it follows from our main result that there are no pointed bubbles for values of $F \neq F_C$. The

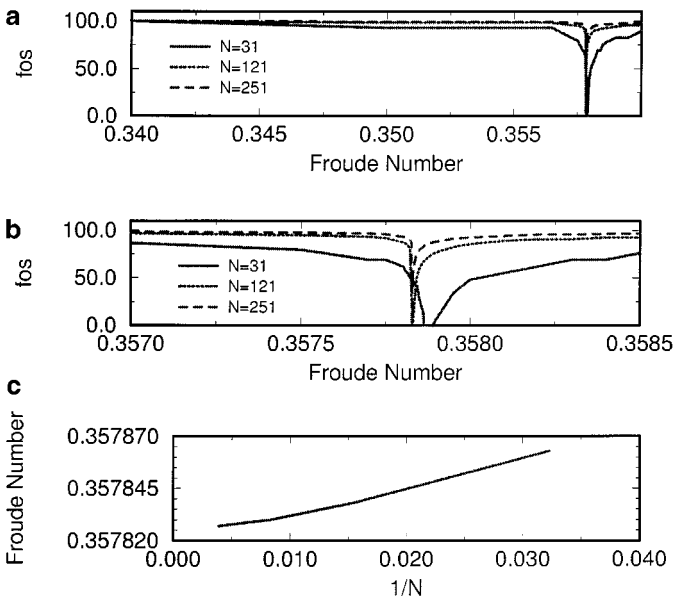


**FIG. 4.** (a) Plots of fos (frequency of oscillations) of the Fourier coefficients, $a_n$ vs $F$ for three different choices of number of Fourier modes $N$ when $\theta_t = 120^\circ$; (b) magnified view of (a) in the sharp transition region; (c) plot of minimum values of $F$ with no oscillations in the Fourier spectrum vs $(1/N)$.

implications are that bubbles at these $F$ (if they exist) are either smooth or cusped bubbles. For more details, see [10].

### 6.2. *Smooth Bubbles*

Numerical experiments used $\theta_t = 180^\circ$ and all discussions in this section are relevant only for this value of $\theta_t$. The solutions are divided into three different regimes below depending on the different qualitative properties of the numerical solutions.

*6.2.1. Regime* $F \le F_1 = 0.234$. Accurate numerical solutions for $F \le F_1$ could be obtained with $N$ as little as 31. Values of the Fourier coefficients obtained with $N = 31$ are accurate up to six decimal places when compared with their values obtained with $N = 121$. Some numerical results are depicted in Figs. 5 and 6.

Figure 5 shows some graphs taken from our computed solutions with $F = F_1$. Figure 5a depicts profiles of the bubbles generated with three different values of $N$. The bubbles are almost indistinguishable. Figure 5b depicts a magnified view of the regions near the apex. These profiles agree with each other remarkably well even at this magnification. The tails of these bubble profiles also agree very well with the theoretical estimate (5.1) as depicted in Fig. 5c. Figure 5d shows a plot of $a_n$ vs $n$. Their amplitudes decay monotonically with increasing $n$ which is not recognizable for values of $n > 50$ (approx.) in this graph.

Figure 6 shows plots of $\ln|a_n|$ vs $\ln n$ for three values of $F$, 0.10, 0.20, and 0.234, indicating that $a_n \sim n^{-1.4}$ as $n \to \infty$, which is found to be independent of $F$ for $F < F_1$.

*These and similar other calculations indicate that qualitative features of all the graphs shown in Figs.* 5 *and* 6 *are generic for all solutions with* $F \le F_1$. *Fourier modal amplitudes* $|a_n|$ *for all these solutions decay monotonically with decay rate* $a_n \sim n^{-1.4}$ (*approx.*) *at large* $n$.

These bubbles are clearly smooth at the apex.

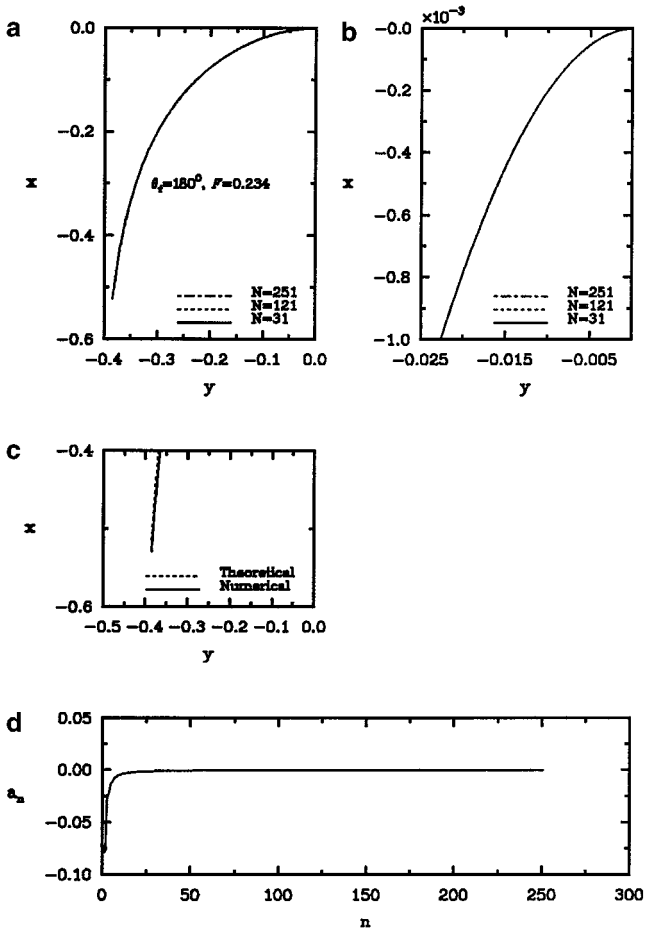


**FIG. 5.** Smooth bubble at $F = 0.234$. (a) Convergence of the bubble profiles; (b) magnified view of the bubble profiles near the tip; (c) comparison of theoretical and numerical shapes of the tails of the bubbles; (d) qualitative behavior of the Fourier spectrum.

*6.2.2. Approximate regime* $F_1 < F \leq 0.30$. We required higher values of $N$ to obtain converged solutions for higher values of $F$. Thus, we could obtain solutions for $F \leq 0.3$ (approx.) with $N = 121$. Some representative solutions in this regime are shown in Figs. 7 and 8.

Figure 7 shows various plots similar to the ones in Fig. 6 but at $F = 0.25$, a slightly higher value than $F_1$. Qualitative aspects of various graphs in this figure are similar to that in Fig. 6

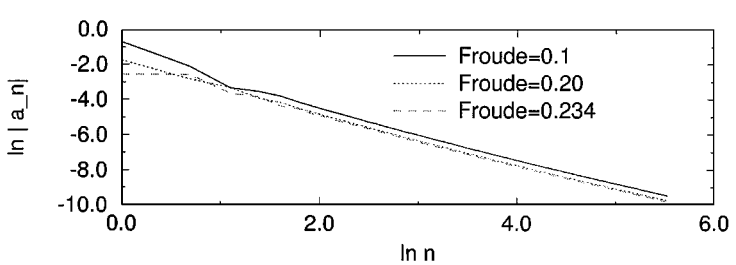


**FIG. 6.** Log–log plots of the Fourier spectrums of solutions obtained with $\theta_t = 180^\circ$ for three values of $F$, 0.1, 0.2, and 0.234 when $N = 251$. The straight line fit has a slope $\simeq -1.4$.

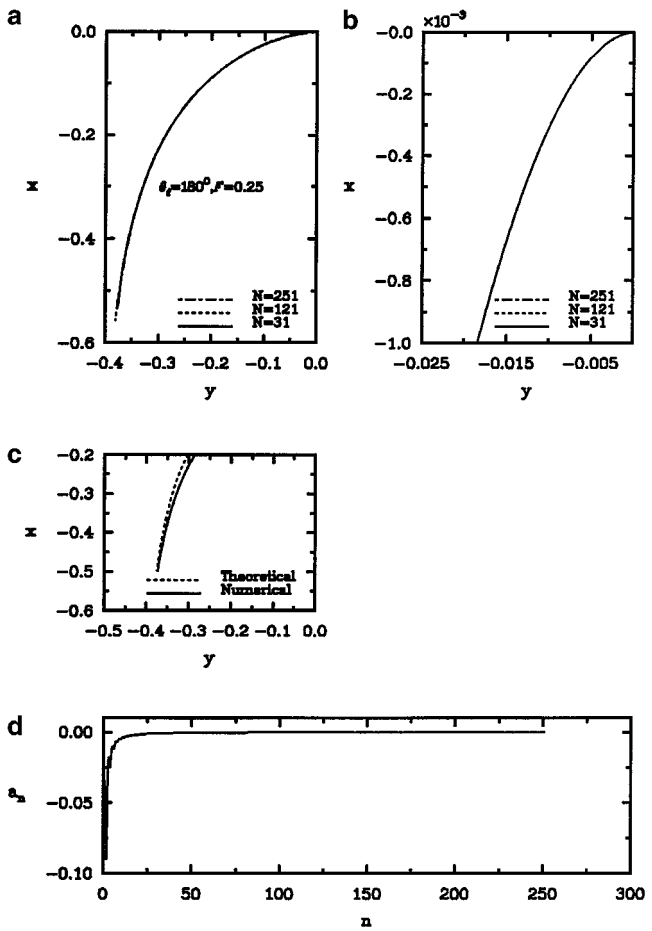


**FIG. 7.** Smooth bubble at $F = 0.25$. (a) Convergence of the bubble profiles; (b) magnified view of the bubble profiles near the tip; (c) comparison of theoretical and numerical shapes near the tails of the bubbles, $N = 251$; (d) qualitative behavior of the Fourier spectrum when $N = 251$.

except for the graph in Fig. 7d. In this figure, oscillations in the Fourier spectrum are clearly visible in the beginning part of the spectrum. These oscillations quickly disappear and the amplitude, thereafter, decreases monotonically.

Figure 8 depicts the plots of $\ln|a_n|$ vs $\ln n$ for three values of $F = 0.236$, 0.27, and 0.29 when $N = 251$. In these figures, oscillations are clearly recognizable whose amplitudes do not differ by more than $10^{-5}$ when calculations with $N = 121$ and $N = 251$ are compared and, hence, are very accurate. These oscillations are not an effect of finite resolution computation. Furthermore, our computations with various values of $N \leq 251$ lead us to believe that Fourier coefficients of the solutions for these values of $F$ will decay monotonically as $n \to \infty$ (see Section 6.2.4 for more details). For all these values of $F$, the asymptotic decay rate remains the same as that for $F < F_1$, i.e., $a_n \sim n^{-1.4}$, as $n \to \infty$. Therefore, it follows from Proposition 1 and our main result that these are smooth bubbles.

It is worthwhile to comment on the appearance of the oscillations as soon as $F$ exceeds $F_1$ whose amplitudes increase with increasing $(F - F_1)$ as seen in this figure. This possibly has to do with the complicated nature of the development of singularity of different order in the complex velocity as $F$ gradually increases towards the transition point where the transition

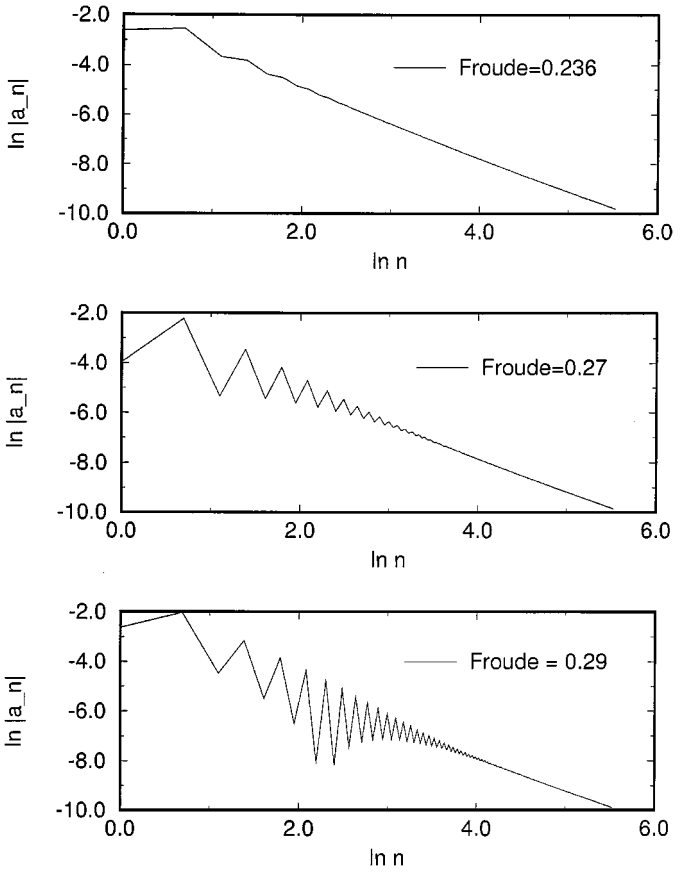


**FIG. 8.** Log–log plots of the Fourier spectrums of solutions obtained with $\theta_t = 180^\circ$ for three values of $F$, 0.236, 0.27, and 0.29 when $N = 251$.

from smooth to pointed topology takes place. This development process probably begins at $F_1$. Since the complex velocity (see (2.2)) has a singularity of order 1 for the smooth bubbles and of order $2/3$ for the pointed bubbles, the function $g(\sigma; \theta_t)$ in (2.2) has to have very awkward dependence on $F$ so that it behaves according to (4.1) as the transition point is approached. Since the Taylor series of the logarithmic term in (4.1) has coefficients which alternate in sign from odd to even mode, the Fourier spectra of the solutions for values of $F$ well before the transition point are likely to show signs of such oscillatory behavior, as is the case here. It is speculated that this awkward dependence begins at $F_1$ and its presence is felt more strongly as $F$ gets closer to the transition point, justifying the nature of oscillations in Fig. 8 with increasing $F$. Of course, it will be desirable to have a suitable expansion of the function $g(\sigma; \theta_t)$ in this regime which will reflect this kind of behavior. However, we have not pursued this yet.

*These and similar other calculations indicate that qualitative features of all the graphs shown in Figs.* 7 *and* 8 *are generic for all solutions with* $F_1 < F < 0.30$ *(approx.). Fourier modal amplitudes* $|a_n|$ *for all these solutions do not decay monotonically at low wavenumbers. But at large wavenumbers, the oscillations disappear and* $|a_n|$ *has an approximate asymptotic decay rate* $a_n \sim n^{-1.4}$.

*6.2.3. Approximate regime $F > 0.30$.* Some representative solutions obtained with $N = 251$ in this regime are discussed next.

The series representation (2.3) becomes really inadequate for the function $g(\sigma)$ and the problem gradually becomes intractable as expected. Some scenarios are presented below.

As $F$ exceeds a value of 0.30, oscillations of very small amplitude of the order of roundoff error first develop at the far end of the Fourier spectrum. At $F = 0.31$, $a_{50} = -6.2 \times 10^{-4}$, $a_{100} = -1.77 \times 10^{-4}$, $a_{150} = -9.7 \times 10^{-5}$, and $a_{200} = -6.6 \times 10^{-5}$. The Fourier coefficients are found to be of one sign for all $a_n$, $n > 31$ and the amplitude of oscillations is of the order of $10^{-7}$.

At $F = 0.33$, $a_{50} = -1.5 \times 10^{-3}$, $a_{100} = -3.8 \times 10^{-4}$, $a_{150} = -1.67 \times 10^{-4}$, and $a_{200} = -9.4 \times 10^{-5}$. The Fourier coefficients are found to be of one sign for all $a_n$, $n > 125$, and the amplitude of oscillations is of $5 \times 10^{-5}$ approximately. As we see, amplitude of these oscillations has increased a little bit but not much.

At $F = 0.34$, $a_{50} = -2.7 \times 10^{-3}$, $a_{100} = -8.3 \times 10^{-4}$, $a_{150} = -4.0 \times 10^{-4}$, and $a_{200} = -2.6 \times 10^{-4}$. The Fourier coefficients now alternate in sign from even to odd $n$ for all $n$ and the amplitude of oscillations is almost of the order of $10^{-4}$ at $n > 200$. Notice that values of the Fourier coefficients decrease slower now than for lower values of $F$.

We also computed with $F = 0.35$ . The solutions are not reliable. The decay rate of the Fourier coefficients seriously deteriorates at $F = 0.35$. For example, $a_{50} = -4.7 \times 10^{-3}$, $a_{100} = -2.0 \times 10^{-3}$, $a_{150} = -1.38.0 \times 10^{-3}$, and $a_{200} = -1.26 \times 10^{-3}$ at this $F$. The Fourier coefficients also alternate in sign from even to odd $n$ for all $n$ and the amplitude of oscillations is almost of the order of $10^{-4}$ for $n > 250$ which is relatively large compared to the Fourier modal amplitudes at large wavenumbers.

Some solutions in this regime are shown later in Section 7.

*Qualitative features of solutions for $F > 0.30$ differ from that for $F_1 < F < 0.30$ in two respects: oscillations appear in the far end of the spectra in our computations with $N$ up to 251 and the decay rate of the Fourier coefficients deteriorates with increasing $F$. Amplitude of the oscillations increases with increasing $F$ which possibly signifies the approach of the transition point.*

*6.2.4. Diagnosis.* Next we characterize the topology at the tips of these bubbles.

Figure 9a displays the frequency of oscillations in the Fourier spectrum as a function of $F$ for three choices of $N$. The sudden emergence of oscillations in the Fourier spectrum is clearly visible as soon as $F$ exceeds a critical value of $F_1$. These oscillations first develop in the the low-wavenumber modes and then propagate towards higher wavenumber modes with increasing $F$ until the entire spectrum is enveloped with persistent oscillations at some $N$-dependent value $F_O(N)$ where $F_1 < F_O(N) < F_C$. For $F \in (F_O(N), F_C)$, all modes participate in this oscillatory behavior. It is worth mentioning here that frequency of oscillations, and *not* the number of oscillations, approaches zero as $N \to \infty$ for $F < F_C$. Actually, the number of oscillations at a fixed $F$ increases with increasing $N$ for $F > F_1$, which should be apparent from this figure.

Figure 9b shows a plot of $F_O(N)$ vs $(1/N)$. This figure clearly suggests that $F_O(N)$ will approach a value above 0.33 as $N \to \infty$. There is obviously some difficulty in predicting the exact limit value from this figure because the linear extrapolation here will not work since the singularity appears to be very complicated as $F$ increases even further. It is my speculation that the limiting value is $F_C$ because as we know from our previous section that a singularity of a different order arises at $F = F_C$ due to the existence of a pointed bubble

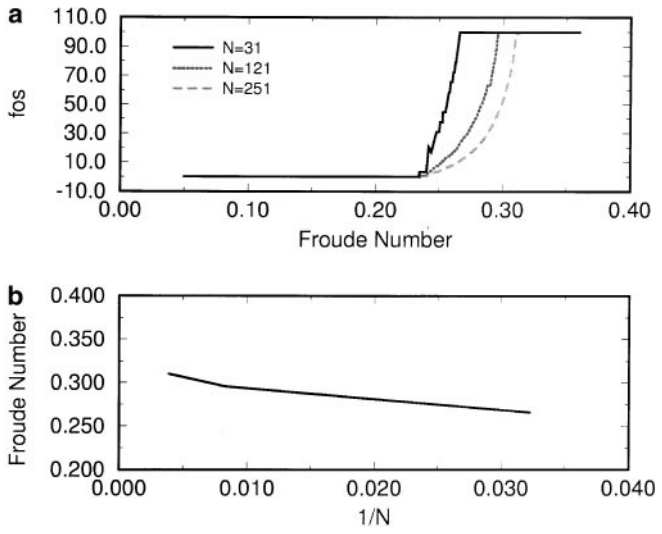


**FIG. 9.** (a) Plots of fos (frequency of oscillations) of the Fourier coefficients, $a_n$ vs $F$ for three different choices of number of Fourier modes $N$; (b) plot of minimum values of $F$ with alternating sign patterns in the sequence $(a_n - a_{n-1})$ against $(1/N)$.

at this value of $F$. *This leads us to conclude that all bubbles in the regime* $0 < F < F_C$ *are probably smooth bubbles.*

Below we show some computations for cusped bubbles, i.e., with $\theta_t = 0$.

### 6.3. *Cusped Bubbles*

Numerical experiments have been carried out with $\theta_t = 0$ for three different values of $N$: 31,121, and 251.

For $F > F_2$ (recall that $F_2 = 0.8$), computed values of $|a_n|$ obtained with $N = 31$ are accurate up to $10^{-6}$ (when compared with their values obtained with $N = 121$) and decay monotonically. For $0.4 < F < F_2$, computed values of $|a_n|$ obtained with $N = 121$ are accurate up to $10^{-5}$ (when compared with their values obtained with $N = 251$) but these do not decay monotonically. Fourier spectra of the solutions develop oscillations which do not disappear with increasing $N$ and are not an effect of discretization. The Fourier coefficients of all these solutions have an asymptotic decay rate $a_n \sim n^{-1.3}$ for all $F > 0.4$. For $F < 0.4$, the oscillations appear more often and solutions are less reliable as $F$ approaches $F_C$ when $N = 251$. Calculations with higher $N$ were not successful. Some fine details of these solutions are depicted below.

Figure 10 shows some graphs taken from our computed solutions at $F = 0.4$. Figure 10a depicts profiles of the bubbles generated with three different values of $N$. The bubbles are almost indistinguishable. Figure 10b depicts a magnified view of the regions near the apex. These profiles agree with each other remarkably well even at this magnification. The tails of these bubble profiles also agree very well with the theoretical estimate (5.1) as depicted in Fig. 10c. Figure 10d shows the graph of the Fourier coefficients $a_n$ against $n$. Their amplitudes decay with oscillations for small wavenumbers which is clearly recognizable for values of $n < 50$ (approx) in this graph. At large $n$, these oscillations do not appear and their amplitudes decay monotonically with $n$.

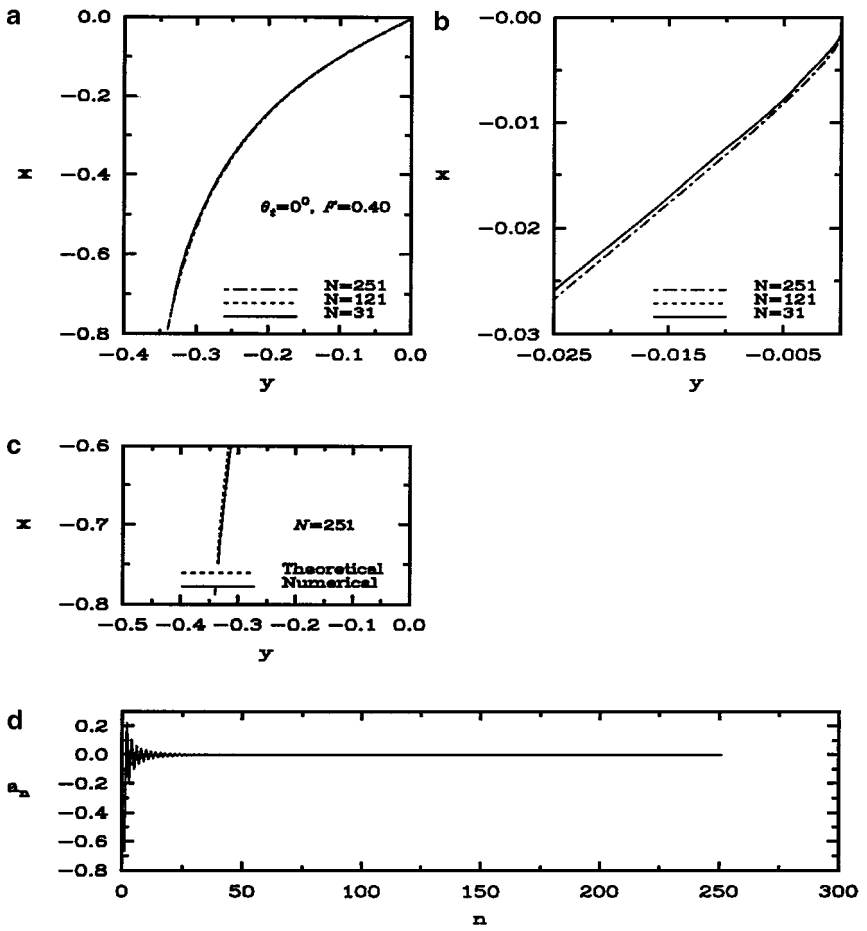


**FIG. 10.** Cusped bubble with $F = 0.4$. (a) Convergence of bubble profiles; (b) magnified view of the bubbles profiles near the tip; (c) comparison of theoretical and numerical shapes of the tails of the bubbles; (d) behavior of the Fourier coefficients.

Figure 11 depicts the plots of $\ln|a_n|$ vs $\ln n$ for three values of $F$: 0.4, 0.6, and 0.7 when $N = 251$. In these figures, the oscillations are clearly recognizable whose amplitudes appear to decrease with increasing $(F - F_C)$. These oscillations do not appear at large wavenumbers. Moreover, these plots indicate that $a_n \sim n^{-1.3}$ as $n \to \infty$ for all these values of $F$. These and similar other calculations appear to suggest that qualitative features of all the graphs shown in Figs. 10 and 11 are generic for all cusped bubbles obtained for values of $F$ in the interval $(0.4, F_2)$. For $F > F_2$, the asymptotic decay rate remains the same, i.e., $a_n \sim n^{-1.3}$ as $n \to \infty$. However, the oscillations in the Fourier spectrum completely disappear for these values of $F$.

Figure 12a displays the frequency of oscillations as a function of Froude number for three choices of $N$. The sudden emergence of oscillations in the Fourier spectrum is clearly visible for $F < F_2$. These oscillations first develop in the low-wavenumber modes as soon as $F$ decreases below $F_2$ and then propagate toward higher wavenumber modes with decreasing $F$ until the entire spectrum is enveloped with oscillations at some $N$-dependent value $F_O(N)$ where $F_C < F_O(N) < F_2$. For $F \in (F_C, F_O(N))$, all modes participate in this oscillatory behavior. As before, it is the frequency of oscillations, and *not* the number of oscillations, that

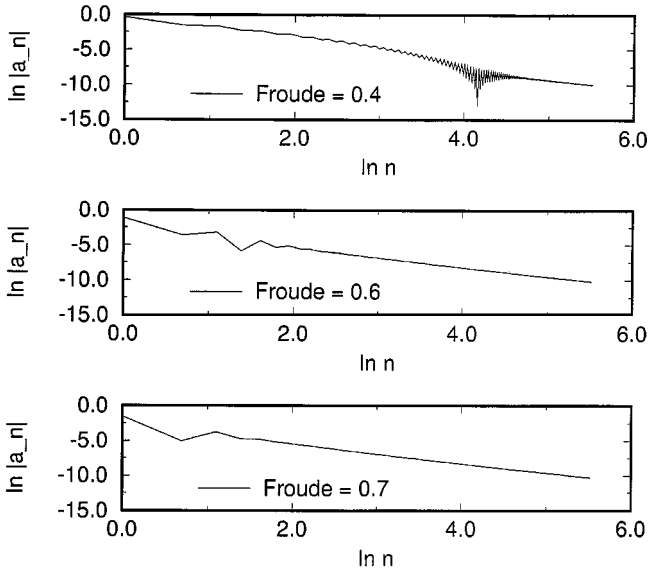


**FIG. 11.** Log–log plots of the Fourier spectrums of solutions obtained with $\theta_t = 0^\circ$ for three values of $F$, 0.4, 0.5, and 0.7 when $N = 251$. It shows a gradual decrease in the frequency of oscillation with an increase in Froude number. The oscillations completely die away at $F \sim 0.8$, not shown here.

approaches zero as $N \to \infty$. The number of oscillations actually increases with increasing $N$ at a fixed $F$ in this regime.

Figure 12b shows a plot of $F_O(N)$ vs $(1/N)$. This figure clearly suggests that $F_O(N)$ very likely approaches $F_C$ as $N \to \infty$. This probably indicates that a singularity in the complex velocity arises as $F \downarrow F_C$. We believe that all bubbles in the regime $F > F_C$ are cusped bubbles and the difficulty with reliable computation for values of $F$ in the

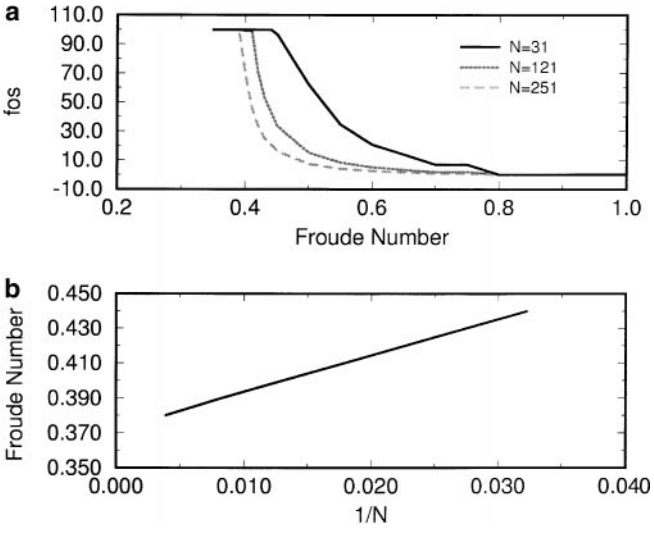


**FIG. 12.** (a) Plots of fos (frequency of oscillations) of the Fourier coefficients, $a_n$ vs $F$ for three different choices of number of Fourier modes $N$; (b) plot of minimum values of $F$ with alternating sign patterns in the sequence $(a_n - a_{n-1})$, against $(1/N)$.

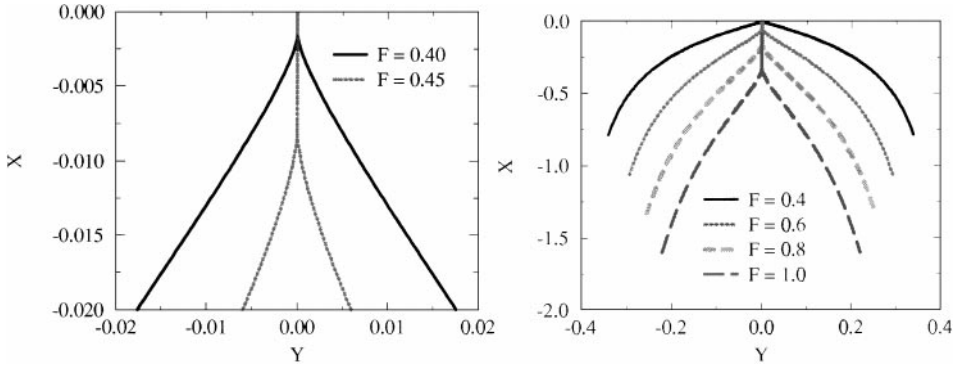


**FIG. 13.** Details near the tip for cusped profiles and the free boundaries at $F = 0.4$, 0.6, 0.8, and 1.

immediate neighborhood of $F_C$ has to do with the very subtle transition from pointed to cusped bubbles.

Figure 13 shows details of the tip for cusped profiles at $F$: 0.4, 0.6, 0.8, and 1.0. The length, $L$, of the stem at the cusp gradually increases with increasing $F$ and approaches infinity as $F \to \infty$. Figure 14 shows a plot of $\ln L$ versus $F$ for $F > 0.4$ and a magnified view of this plot for $F > 0.75$. The symbol ● in this figure shows actual data points. The data points for $F > 0.75$ fit into the following equation within an error of 1%,

$$L = A\, e^{mF}, \tag{6.1}$$

where $A = 0.6357$ and $m = 0.351$.

## 7. TOPOLOGY TRANSITION

The transition scenario from pointed to smooth (cusped) bubbles as $F$ decreases below (increases above) $F_C$ is a very subtle issue due to the possible complicated nature of the singularity alluded to in previous sections. This is reflected in numerical difficulties for values of $F$ close to $F_C$.

Figure 15 shows the bubble profiles including the magnified view of the region near the tip (see the right box in the figure) for several values of $F$: 0.31, 0.33, $F_C$, 0.4. These

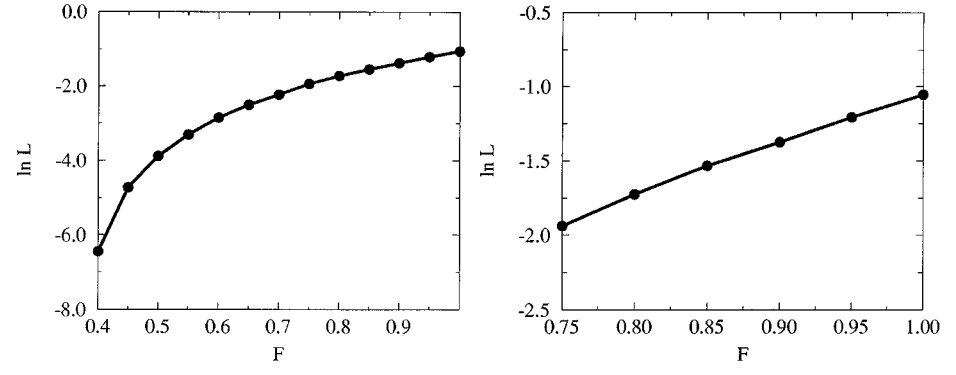


**FIG. 14.** The $\ln L$ vs $F$ plot and its magnified view for $F > 0.75$.

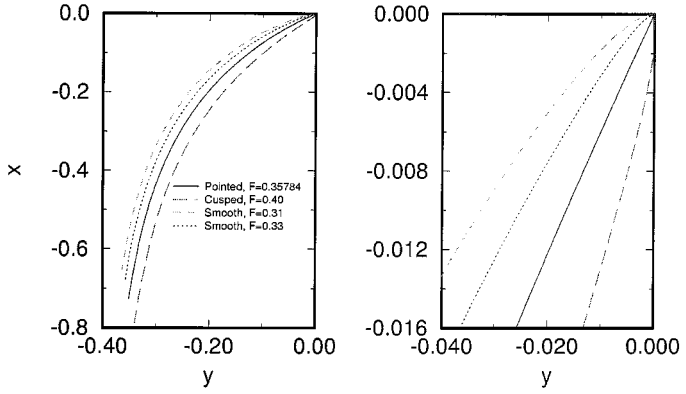


**FIG. 15.** Left, bubble profiles at four values of $F$, 0.31, 0.33, 0.35784, and 0.4. Right, the profiles near the tip of these bubbles.

results were obtained with $N = 251$. From this figure, the following scenario of topological transition at $F = F_C$ emerges. A rounded nose of vanishing size appears at the tip as soon as $F$ decreases below (increases above) $F_C$. The radius of curvature of this nascent smooth profile at the tip gradually increases with decreasing $F$ (and approaches infinity as $F \to 0$ which corresponds to a flat interface separating the heavy liquid from the gas). Similarly, a cusp of vanishing size appears at the tip as soon as $F$ exceeds $F_C$.

It will be worthwhile to test the validity of the above transition scenario by a more suitable numerical method.

## 8. DISCUSSIONS AND CONCLUSIONS

In this paper, we have characterized the topology at the tip of the bubbles based on the limit behavior of the qualitative properties of the Fourier spectra of numerical solutions. We have presented a systematic study of the dependence of $F$ on $\theta_t$ and have presented some evidence which seems to indicate that the bubbles with $F < F_C$ are smooth, the bubbles with $F = F_C$ are pointed, and the bubbles with $F > F_C$ are cusped.

Due to the inadequacy of the series representation (2.3) for finding very accurate solutions in the immediate neighborhood of the transition point $F_C$, we have used our main results, i.e., the asymptotic properties of the qualitative behavior of the Fourier spectra of the solutions. It will be desirable to verify the numerical results presented here with results obtained using another approach which can handle the complicated nature of the singularities alluded to in this paper.

In this connection, an approach would be to consider the inclusion of singular terms outside the unit disk, i.e., outside the region of interest, for smooth but nearly pointed bubbles and consider their dynamics in the complex plane as the parameter $F$ is varied. One or more of such singularities will hit the unit disk exactly at the critical speed, $F_C$, where the smooth bubble turns pointed. This approach for studying singularity formation in other moving free boundary problems has been used by many researchers including Longuet-Higgins [21], Howison *et al.* [16–18], Peterson [24], Tanveer [25], Baker *et al.* [1] among many others. However, use of this approach for determining the critical speed $F_C$ for this bubble problem is still open and remains a topic of future research. Results obtained using this approach can also serve to partially validate the numerical results presented here.

In closing, we would like to make the following remarks.

• At first sight, different limiting behaviors (4.1) and (4.2) at $F_C$ appear quite awkward and could be the source of numerical difficulties as we have noticed before. It will be desirable to have an asymptotic theory in the vicinity of the transition which will undoubtedly require the technique of asymptotics beyond all orders [20, 25, 26, 5, 6]. This might also give some insight into the nature of complexity of the singularity at the tip and may even be able to provide more accurate numerical methods for this problem.

• It is worth mentioning here that the surface tension acts as a destabilizing force in this problem because the zero surface tension limit bubble has a speed close to $F_1 = 0.234$ which is much (more than 50%) lower than the speed, $F_C = 0.35784$, of the fastest zero surface tension bubble.

• We should note that Garabedian [13] used only the first four terms of a uniformly valid asymptotic expansion of the flow and obtained a lower bound of the fastest speed to be equal to 0.2363. Perhaps, with more accurate calculations without neglecting too many terms in the asymptotic expansion one could obtain the speed of the fastest smooth bubble close to the one obtained here. It may also be worth investigating this approach of Garabedian.

## ACKNOWLEDGMENTS

I thank the anonymous reviewers for their helpful suggestions. This paper is based in part upon work supported by the Texas Advanced Research Program (Grant TARP-97010366-030). This research is also partly supported by the Interdisciplinary Research Program of the Office of the Vice President for Research and Graduate Studies at Texas A&M University. The allocation of computer resources by the Texas A&M Supercomputer Center is gratefully acknowledged.

## REFERENCES

1. G. Baker, R. Caflisch, and M. Siegel, Singularity formation during Rayleigh–Taylor instability, *J. Fluid Mech.* **252**, 51 (1993).
2. G. Birkhoff, *Taylor Instability and Laminar Mixing*, Los Alamos Report LA-1862 (1954), p. 1.
3. G. Birkhoff, *Taylor Instability, Appendices to Report LA-1862*, Los Alamos Report LA-1927 (1956), p. 1.
4. G. Birkhoff and D. Carter, Rising plane bubbles, *J. Math. Phys.* **6**, 769 (1957).
5. R. Combescot, T. Dombre, V. Hakim, Y. Pomeau, and A. Pumir, Shape selection for Saffman–Taylor fingers, *Phys. Rev. Lett.* **56**, 2036 (1986).
6. R. Combescot, T. Dombre, V. Hakim, Y. Pomeau, and A. Pumir, Analytic theory of the Saffman–Taylor fingers, *Phys. Rev. A* **37**, 1270 (1988).
7. B. Coüet, G. Strumolo, and A. E. Dukler, Modelling two-dimensional large bubbles in a rectangular channel of finite width, *Phys. Fluids* **29**, 2367 (1986).
8. B. Couët and G. S. Strumolo, The effects of surface tension and tube inclination on a two-dimensional rising bubble, *J. Fluid Mech.* **184**, 1 (1987).
9. P. Daripa, A numerical investigation of some pattern selection issues in the rising plane Taylor–bubble problem, *J. Comput. Phys.* **121**(1), 129 (1995).
10. P. Daripa, Pointed Taylor bubble revisited, *J. Comput. Phys.* **123**(1), 226 (1996).
11. R. M. Davies and G. I. Taylor, The mechanics of large bubbles rising through extended liquids and through liquids in tubes, *Proc. R. Soc. London Ser. A* **200**, 375 (1950).
12. C. Domb and M. F. Sykes, On the susceptability of a ferromagnetic above the Curie point, *Proc. R. Soc. London Ser. A* **240**, 214 (1957).

13. P. R. Garabedian, On steady-state bubbles generated by Taylor instability, *Proc. R. Soc. London Ser. A* **241**, 423 (1957).
14. P. R. Garabedian, A remark about pointed bubbles, *Comm. Pure Appl. Math.* **38**, 609 (1985).
15. P. R. Garabedian, Private Communication, November 1996.
16. S. D. Howison, J. R. Ockendon, and A. A. Lacey, Singularity development in moving-boundary problems, *Quart. J. Mech. Appl. Math.* **38**(3), 343 (1985).
17. S. D. Howison, Fingering in Hele–Shaw cells, *J. Fluid Mech.* **167**, 439 (1986).
18. S. D. Howison, A. A. Lacey, and J. R. Ockendon, Nonuniqueness in singular viscous fingering, Hele–Shaw free-boundary problems with suction, *Quart. J. Mech. Appl. Math. II* **41**, 183 (1988).
19. D. A. Kessler and H. Levine, Velocity selection for Taylor bubbles, *Phys. Rev. A* **39**, 5462 (1989).
20. M. D. Kruskal and H. Segur, Asymptotics beyond all orders in a model of crystal growth, *Stud. Appl. Math.* **85**, 129 (1991).
21. M. S. Longuet-iggins, On the forming of sharp corners at a free surface, *Proc. R. Soc. London Ser. A* **371**, 453 (1980).
22. D. W. Moore, The spontaneous appearance of a singularity in the shape of an evolving vortex sheet, *Proc. R. Soc. London Ser. A* **365**, 105 (1979).
23. D. W. Moore, Numerical and analytical aspects of Helmholtz instability, in *Theoretical and Applied Mechanics*, edited by F. I. Niordoson and N. Olhoff (Elsevier, Amsterdam/New York, 1985).
24. M. A. Peterson, Nonuniqueness in singular viscous fingering, *Phys. Rev. Lett.* **62**, 284 (1989).
25. S. Tanveer, Viscous displacements in a Hele–Shaw cell, in *Asymptotics Beyond All Orders*, edited by H. Segur, S. Tanveer, and H. Levine, NATO ASI Series B, Physics (Plenum, New York, 1991), Vol. 284.
26. S. Tanveer, Analytic theory for the selection of Saffman–Taylor finger, *Phys. Fluids* **30**, 1589 (1987).
27. G. I. Taylor, The instability of liquid surfaces when accelerated in a direction perpendicular to their planes, I, *Proc. R. Soc. London Ser. A* **201**, 192 (1950).
28. J.-M. Vanden-Broeck, Bubbles rising in a tube and jets falling from a nozzle, *Phys. Fluids* **27**, 1090 (1984).
29. J.-M. Vanden-Broeck, Rising bubbles in a two dimensional tube with surface tension, *Phys. Fluids* **27**, 2604 (1984).
30. J.-M. Vanden-Broeck, Pointed bubbles rising in a two dimensional tube, *Phys. Fluids* **29**, 1343 (1986).
31. M. Van-Dyke, Computer-extended series, *Ann. Rev. Fluid Mech.* **16**, 287 (1984).
32. A. Zygmund, *Trigonometric Series* (Cambridge Univ. Press, Cambridge, UK, 1968), Vol. 1.